

Dynamical diffraction peak splitting in time-of-flight neutron diffraction

E. Üstündag^{a)}

Department of Materials Science and Engineering, Iowa State University, Ames, Iowa 50011

R. A. Karnesky

Department of Materials Science and Engineering, Northwestern University, Evanston, Illinois 60208

M. R. Daymond

Department of Mechanical and Materials Engineering, Queen's University, Kingston, Ontario K7L3N6, Canada

I. C. Noyan

Department of Applied Physics and Applied Mathematics, Materials Science Program, Columbia University, New York, New York 10027

(Received 16 May 2006; accepted 3 November 2006; published online 8 December 2006)

Time-of-flight neutron diffraction data from 20 and 0.7 mm thick perfect Si single crystal samples, which exhibit dynamical diffraction effects associated with finite crystal size, are presented. This effect is caused by constructive interference occurring solely from thin layers bounded by the front (entry) and back (exit) surfaces of the sample with no scattering originating from the layers in between, resulting in two distinct peaks observed for each reflection. If the sample is thin and/or the instrument resolution is insufficient, these two peaks can convolve and cause peak shape aberrations which can lead to significant errors in the strain and peak-broadening parameters obtained from a kinematical diffraction analysis. © 2006 American Institute of Physics. [DOI: 10.1063/1.2402220]

In spallation-neutron-source-based powder diffractometers utilizing the time-of-flight (TOF) principle,¹ the convolution of the time structure of the pulsed source and the neutron flight path introduce significant asymmetries into the incident beam profile, which, when convolved with the diffraction profile of the sample, result in asymmetric diffraction peaks across the entire range of Bragg angles. These asymmetries are strong enough that the position of the observed intensity maximum can be quite different from the actual angle (or the corresponding TOF) for the Bragg reflections, and thus, peak profile fitting is required to determine the true plane spacing. The coefficients that cause such asymmetry are generally obtained from data refinements of standard reference materials.

It is not clear how well the profile functions employed in TOF neutron powder diffraction data analysis^{2,3} represent TOF data from single crystals, or from coarse grained specimens. In these cases additional peak asymmetry may be caused by dynamical diffraction effects and the strain values computed with peak-fitting programs based on kinematical diffraction approximations might be erroneous. These issues are of practical interest since the beam sizes used on neutron diffractometers are decreasing: new instrument development will soon introduce neutron beam sizes as small as 100 μm .⁴ Furthermore, attempts have been recently made to employ current neutron powder diffractometers in residual strain measurements of large single crystal specimens. The present investigation was designed to check for these effects in two state-of-the-art TOF neutron powder diffractometers.

The samples used in this study were semiconductor-grade Si single crystal cylinders, approximately 100 mm in diameter, with the [001] direction parallel to the cylinder axis, with thicknesses of 20 and 0.7 mm, respectively. Two

spallation-neutron powder diffractometers, SMARTS⁵ at the Los Alamos Neutron Science Center and ENGIN X⁶ at the ISIS Neutron Facility, Rutherford Appleton Laboratory (UK), were utilized. In all cases, the sample was mounted at approximately $\theta=45^\circ$ to the incoming neutron beam (Fig. 1). On SMARTS, the entire TOF diffraction data were collected from all of the detectors (192 tubes) of bank 1 [Fig. 1(a)]. These data were time focused as described in Ref. 1; the time focusing assures that the correct d spacing is obtained from individual detectors as well as the whole bank by taking into account TOF differences between different detectors. On ENGIN X, which is a higher resolution instrument, a shield was placed in front of the bank 2 detectors that had only a single 5 mm wide opening at $2\theta=-88.43^\circ$ [Fig. 1(b)]. The intersection of this aperture with the 10 mm high, 5 mm wide [in the plane of the drawing of Fig. 1(b)] incident beam defined the sampling volume seen by the exposed detector(s). The sample was then traversed across this sampling volume in 2 mm steps along its surface normal to obtain a depth profile of the diffraction data.

The diffraction data from both instruments revealed unexpected features when interpreted with kinematical diffraction assumptions. Figure 2 shows the observed TOF profile from bank 1 detectors of the SMARTS diffractometer. The data from the 20 mm thick specimen contain two reflections: a strong peak at $d_1 \cong 1.3509 \text{ \AA}$ with (full width at half maximum) $\text{FWHM}_1 \cong 0.0054 \text{ \AA}$ and another peak with approximately 50% of the intensity of the first one at $d_2 \cong 1.3648 \text{ \AA}$, with $\text{FWHM}_2 \cong 0.0046 \text{ \AA}$, instead of the expected single peak for the Si 004 reflection at approximately 1.3577 \AA . These peaks are not fully resolved in the diffracted intensity profile of the thinner specimen; fitting two peaks to the observed profile yields $d_1 \cong 1.3585 \text{ \AA}$, $\text{FWHM}_1 \cong 0.0044 \text{ \AA}$ and $d_2 \cong 1.3548 \text{ \AA}$, $\text{FWHM}_2 \cong 0.0037 \text{ \AA}$, respectively. Using kinematical diffraction concepts, these data would indicate that both samples are bicrystals, with each

^{a)}Electronic mail: ustundag@iastate.edu

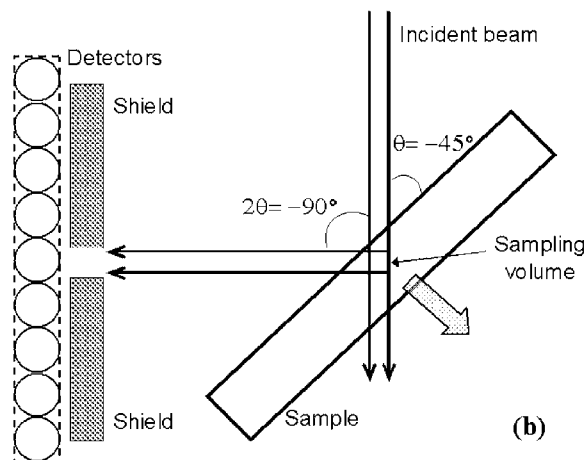
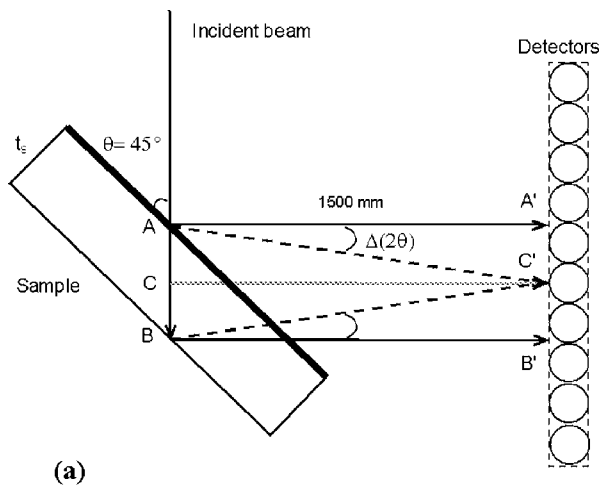


FIG. 1. Schematic of the diffraction geometry on SMARTS (a) and ENGIN X (b) for the 20 mm thick Si specimen; not to scale. The specimens were placed at about $\pm 45^\circ$ to the incident neutron beam. The 0.7 mm thick specimen was run similarly on SMARTS. The diffraction data were collected by the $2\theta = \pm 90^\circ$ detector banks. Points A', B', and C' define the positions the volumes at A, B, and C (the diffractometer center) would scatter into the SMARTS detectors at $2\theta \sim 90^\circ$. On ENGIN X, the sampling volume was defined by the intersection of the 10 mm (height) by 5 mm (width, in the plane of the drawing) incident neutron beam and the 5 mm wide receiving slit. The sample was then translated in 2 mm steps along its surface normal such that various depths were interrogated.

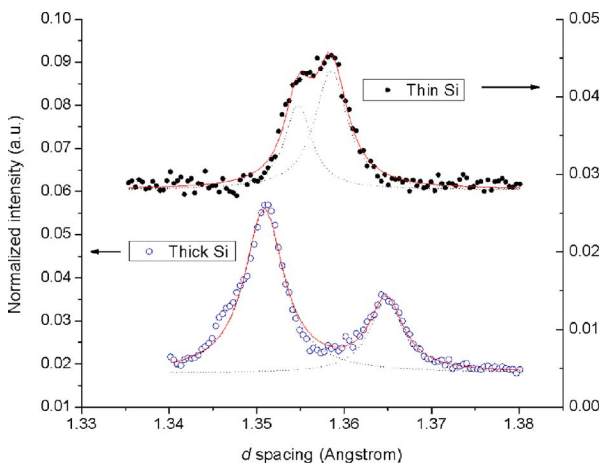


FIG. 2. (Color online) Time focused Si 004 reflection data obtained on SMARTS from the complete $2\theta = +90^\circ$ bank (bank 1) detectors for the 20 and 0.7 mm thick Si samples.

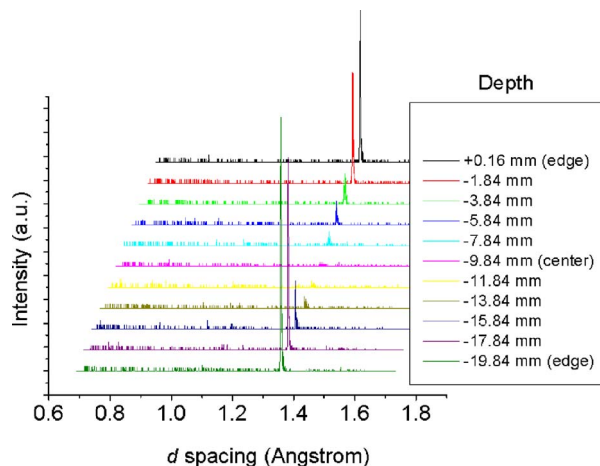


FIG. 3. (Color online) Results of the depth scan on ENGIN X of the 20 mm thick Si specimen. The data were collected in one detector element at $2\theta = -88.43^\circ$. The Si 004 peak intensity is seen to exist near each sample edge, yet it disappears at the sample center.

section having a different composition or strain. Assuming that differences are strictly due to strain, the absolute strain differences between the two regions would be about 0.01 for the thicker sample and 0.003 for the thinner sample. These strain values would correspond to stresses comparable to the fracture strength of single crystal Si at room temperature (0.3–7 GPa).⁷ In addition, we had mapped both surfaces of the Si wafers using x-ray diffraction before the neutron experiments and had not observed any indication of bicrystallinity.

The data from the depth-resolved neutron TOF diffraction scans performed on ENGIN X with the thicker sample are shown in Fig. 3. In this figure, each trace corresponds to the TOF data originating from a different depth in the sample. We observe two well-separated peaks, which originate from the front and back near-surface regions of the specimen, respectively, while no diffracted intensity is obtained from the Si between these two regions. Both of these peaks have the same d spacings (~ 1.3581 and 1.3579 Å, respectively) which are quite close to the expected Si 004 plane spacing of 1.3577 Å. The intensity of the diffraction peak from the back of the sample ($x = 0.16$ mm) is $\sim 60\%$ of that from the front surface ($x = -19.84$ mm). This neutron diffraction signature (i.e., two peaks with nearly the same plane spacing originating from the front and back surfaces, with no intensity from the material in between, and with the back surface peak weaker in intensity due to absorption) is indicative of dynamical front-face and back-face diffractions in the Bragg-Bragg geometry where the incident and diffracted beams enter and leave the crystal without encountering any lateral (side) surfaces.^{8,9} This effect is quite well known in steady-state (constant wavelength) neutron interferometers, where the reflection from the back face must be blocked to obtain good peak profiles.^{10,11} It has not been reported before in TOF neutron diffraction.

The discrepancy between the SMARTS and ENGIN X data is due to the different experimental conditions. In SMARTS [Fig. 1(a)] the two peaks originate from different depths and fall on two different detectors; two dynamically diffracting regions at each surface (their thickness is about $60 \mu\text{m}$, given by the extinction depth for Si 004 in this geometry) act as two separate specimens displaced by about

14 mm from the diffractometer center [point *C* in Fig. 1(a)]. The *d* spacing difference between either surface and the center that will result due to this displacement can be calculated using the following equation:¹²

$$\frac{\Delta d}{d} = \frac{\Delta t}{t} - \frac{\Delta L}{L} - \Delta\theta \cot \theta. \quad (1)$$

Equation (1) is obtained from the differentiation of Bragg's law for TOF neutron diffraction.¹³ Here, the first term that contributes to the *d* spacing error is the TOF (*t*) broadening of the moderator,⁶ which for the Si 004 peak on SMARTS is about 6.1×10^{-4} . This term is independent of the sample (but it does depend on the reflection considered). The second term is due to the flight path difference (ΔL) between the points *A* or *B* and *C* in Fig. 1(a). The last term is the error due to the displacement of the diffraction volume elements (points *A* or *B*) from the diffractometer center (point *C*). Using Eq. (1), the difference in *d* spacing between the front- and back-surface peaks, $(\Delta d)_{A-B}$ in terms of the diffraction angle θ , the sample thickness t_s , the sample-to-detector distance R_G , and the nominal plane spacing *d*, is given by

$$(\Delta d)_{A-B} \cong \frac{t_s d}{\cos \theta} \left(\frac{1}{L} + \frac{\cot \theta}{2R_G} \right). \quad (2)$$

This equation is obtained by writing Eq. (1) for the points *A* and *B*, computing the difference, and then expressing the path difference in terms of the specimen thickness and geometry. As expected, the error scales linearly with the sample thickness and inversely with total flight path ($L \sim 33.5$ m on SMARTS) and sample-to-detector distance ($R_G \sim 1.5$ m on SMARTS). Assuming that point *C* corresponds to the actual center of the diffractometer, the absolute plane spacing difference between the front and back faces of the 20 mm wafer (at *A* and *B*) is estimated at approximately 0.013 Å, which is quite close to the observed value of about 0.01 Å. For the 0.7 mm thick specimen, Eq. (2) yields $(\Delta d)_{A-B} \cong 5.2 \times 10^{-4}$ Å, which is an order of magnitude smaller than the difference observed experimentally: 3.7×10^{-3} Å. However, this discrepancy is due to the limited resolution of the instrument: if we set the sample thickness equal to the 10 mm diameter of the individual detector elements used in SMARTS, we observe reasonable agreement between the predicted and observed errors.¹⁴ Sample position and the errors associated with the diffracting volume locations do not apply to the ENGIN X experiment [Fig. 1(b)]; here the sample was moved such that the diffracting volume seen by the detector was always over the diffractometer center. Therefore, the *d* spacing of the Si 004 peak remained unchanged.

The effects described above show that back-face Bragg diffraction can seriously impair the accuracy and precision of parameters obtained from neutron diffraction spectra of specimens with crystallite size comparable to or larger than the neutron extinction depth. In such cases, double peaks, peaks with shoulders, or asymmetric peaks cannot be uniquely ascribed to bicrystals, twins, strain and/or composition gradients, or multiple phases within the diffracting volume. Whether the front and back surface peaks are resolved or add up to form a broadened peak depends on the intrinsic

resolution of the instrument, the diffraction geometry, and on the sample thickness, as illustrated by the data in Fig. 2. Several methods can be utilized to verify if the effects observed are due to dynamical diffraction artifacts. (i) One can use the configuration shown in Fig. 1(b) and scan the beam across the diffracting volume to see if the characteristic back-face diffraction pattern (Fig. 3) is observed. (ii) Alternatively, one can calculate the expected beam profile using dynamical theory.^{11,15} Finally, (iii), for a perfect crystal one can rotate the specimen 180° and reacquire the diffraction data. If the weak and strong peaks switch position, the effect is not due to dynamical diffraction.

In summary, dynamical diffraction processes can cause artifacts, such as double peaks, peaks with shoulders, or highly asymmetric peaks for single crystal or very-large grained polycrystalline specimens examined in TOF neutron powder diffractometers. Unless they are properly identified, such artifacts can cause large errors in data analysis and interpretation.

Funding was provided by the National Science Foundation (NSF) grants DMR-9985264 and IMR-MIP DMR-0412074. The authors acknowledge help from Dr. B. Clausen at the Los Alamos Neutron Science Center which is supported by the U.S. Department of Energy under Contract No. W-7405-ENG-36. The ENGIN-X diffractometer is located on the ISIS Pulsed Neutron Facility, Rutherford Appleton Laboratory, UK, where author M.R.D. was a staff member during the experiments.

¹J. D. Jorgensen, J. Faber, J. M. Carpenter, R. K. Crawford, J. R. Haumann, R. L. Hitterman, R. Kleb, G. E. Ostrowski, F. J. Rotella, and T. G. Worlton, *J. Appl. Crystallogr.* **22**, 321 (1989).

²W. I. F. David and J. D. Jorgensen, *The Rietveld Method*, edited by R. A. Young (Oxford University Press, Oxford, 1995), pp. 197–226.

³R. B. Von Dreele, J. D. Jorgensen, and C. G. Windsor, *J. Appl. Crystallogr.* **15**, 581 (1982).

⁴G. E. Ice, C. R. Hubbard, B. C. Larson, J. W. L. Pang, J. D. Budai, S. Spooner, S. C. Vogell, R. B. Rogge, J. H. Fox, and R. L. Donabarger, *Mater. Sci. Eng., A* **437**, 120 (2005).

⁵M. A. M. Bourke, D. C. Dunand, and E. Üstündag, *Appl. Phys. A: Mater. Sci. Process.* **74**, S1707 (2002).

⁶M. W. Johnson and M. R. Daymond, *J. Appl. Crystallogr.* **35**, 49 (2002); J. A. Dann, M. R. Daymond, L. Edwards, J. A. James, and J. R. Santisteban, *Physica B* **350**, 511 (2004).

⁷S. M. Hu, *J. Appl. Phys.* **53**, 3576 (1982).

⁸C. G. Shull, *J. Appl. Crystallogr.* **6**, 257 (1973).

⁹A. Zelinger, C. G. Shull, J. Arthur, and M. A. Horne, *Phys. Rev. A* **28**, 487 (1983).

¹⁰M. Agamalian, G. D. Wignall, and R. Triolo, *J. Appl. Crystallogr.* **30**, 345 (1997).

¹¹M. Agamalian, E. Iolin, L. Rusevich, C. J. Glinka, and G. D. Wignall, *Phys. Rev. Lett.* **81**, 602 (1998).

¹²C. G. Windsor, *Pulsed Neutron Scattering* (Taylor & Francis, London, 1981), p. 232.

¹³In Eq. (1) the changes in θ and L are correlated. Therefore, the complete differential form, maintaining the signs is needed to calculate a true change in lattice plane spacing.

¹⁴Equation (2) does not take into account any instrument parameters that contribute to the “width” of the peaks from the front and/or back faces. It does not also take into account the possibility of anomalous transmission of the incident neutrons (perpendicular to the sample surface) which would cause the separation between the two peaks to be even smaller for the 0.7 mm thick specimen. For the 20 mm specimen we do not expect anomalous transmission, and did not observe any.

¹⁵H. Yan and I. C. Noyan, *J. Appl. Phys.* **98**, 073527 (2005).